Quasiparticle band structure for the Hubbard systems: Application to α-$CeAl_2$

J. Costa-Quintana and F. López-Aguilar
Departamento de Física, Grupo de Electromagnetismo, Universidad Autónoma de Barcelona, Bellaterra, E-08193 Barcelona, Spain

S. Balle
Departament de Física, Universitat de les Illes Balears, E-07071 Palma de Mallorca, Spain

R. Salvador
Control Data Corporation and Supercomputer Computations Research Institute, Florida State University, Tallahassee, Florida 32306-4052

(Received 12 June 1989; revised manuscript received 6 October 1989)

A self-energy formalism for determining the quasiparticle band structure of the Hubbard systems is deduced. The self-energy is obtained from the dynamically screened Coulomb interaction whose bare value is the correlation energy U. A method for integrating the Schrödingerlike equation with the self-energy operator is given. The method is applied to the cubic Laves phase of α-$CeAl_2$ because it is a clear Hubbard system with a very complex electronic structure and, moreover, this system provides us with sufficient experimental data for testing our method.

I. INTRODUCTION

The spectrum of the electron gas can be obtained by considering approximations to the exchange and correlation by means of local and static potentials. This simplified model—called the local-density formalism (LDF)—has been successful in the description of the ground state of some semiconductors and metals whose valence and conduction band states have effective masses similar to that of the free electron. However, when the valence and/or conduction electrons of the material are more localized, the electronic correlation is such that the LDF do not draw the features of the electronic structure of these compounds and cannot reproduce their physical properties.[1-10]

The Hubbard systems (HS) (or narrow-band systems) constitute a subject of intensive research since the heavy-fermion metals (HFM) and mixed valence compounds (MVC) are explained with the narrow-band Hamiltonian.[1,2,11-19] These systems present intriguing anomalies in their physical properties (electronic specific heat, magnetic susceptibility, electrical resistivity, etc.)[20-33] which arise from the strong correlation between their f electrons. The static local potentials lead to two main failures which are considered in the calculation of the HFM-MVC electronic structures: (i) The density of states presents a single f peak, whose width is about 1(2) eV for all $4f(5f)$ systems. This result contradicts the direct and inverse x-ray photoemission spectroscopies (XPS) which display three or four f peaks clearly split.[20-27] In addition, the splittings, locations, and widths of these peaks are quite different for the different compounds. (ii) The experimental electronic specific heat of these systems is between 5 and 1000 times larger than that resulting from the LDF.[28-34] This fact implies that the effective mass enhancement of the electrons close to the Fermi level is such that the many-body effects have to be considered using dynamical and nonlocal potentials since this mass enhancement is given by[28-34]

$$\frac{m^*}{m_{\mathrm{LDF}}} = \left| 1 - \left(\frac{\partial \Sigma}{\partial \omega} \right)_{\omega = \mathrm{pole}} \right| .$$

As point (ii) states clearly, these systems suffer important dynamical effects for energies close to the Fermi level.[11-18] Therefore, the basic issue for understanding the properties of the HS is to know their quasiparticle spectrum which is constituted by narrow-band resonances located around E_F.[11-18,20-27] These resonances produce the anomalous behavior of the electronic specific heat, the electrical resistivity, and magnetic susceptibility.[28-33] The structure of these resonances, their locations, heights of the peaks, etc., can only be determined from a self-energy band structure formalism. The objective of this paper is to elaborate this formalism for those systems which present narrow-band phenomena and are behind the Mott condition, i.e., $\delta < U$, δ and U being the width of the active band and the Coulomb correlation energy of the electrons in this band, respectively. In recent papers,[1,2,19] second order approximations for the self-energy have been used in cases with nondegenerated bands in order to explain some properties of the electronic structure of the HFM. Nevertheless, the large U requires an infinite order perturbation series in the self-energy, which can be achieved by means of a dynamically screened interaction. The self-energy band structure method presented in this work considers an infinite order self-energy operator deduced with the so-called Green function-W interaction (GW) approximation[34] and the corresponding Schrödingerlike equation with the dynamic and nonlocal potential is solved within the augmented-plane-wave (APW) method.

II. SELF-ENERGY SCHRÖDINGERLIKE EQUATION

We start from the self-energy functional[34]

$$\Sigma(\mathbf{r},\mathbf{r}',\omega)=\Sigma_H(\mathbf{r},\mathbf{r}')+\Sigma_{\mathrm{GW}}(\mathbf{r},\mathbf{r}',\omega)\ , \tag{1}$$

where Σ_H is the Hartree term, which in the Hubbard model reads

$$\Sigma_H(\mathbf{r},\mathbf{r}')=Un\sum_f f(\mathbf{r})f^*(\mathbf{r}')\ , \tag{2}$$

n being the f electron count which should be calculated self-consistently. The $f(\mathbf{r})$ functions are orbtials whose radial parts can be determined either by the renormalized atom approach (RAA) or by any alternative method which allows us to obtain f orbitals for different energies.

The term Σ_{GW} is the GW approximation to the self-energy, which for the multiband Hubbard system reads

$$\Sigma_{\mathrm{GW}}(\mathbf{r},\mathbf{r}',\omega)=\sum_{f,f'} M_{ff'}(\omega)f(\mathbf{r})f'^*(\mathbf{r}')\ , \tag{3}$$

where

$$M_{ff'}(\omega)=\frac{i}{N}\sum_{\mathbf{k},\alpha,\beta}\int_{-\infty}^{+\infty}\frac{d\omega'}{2\pi}e^{i\omega'0^+}\langle f|\mathbf{k}\alpha\rangle\langle\mathbf{k}\beta|f'\rangle W(\omega')G_{\alpha\beta}(\mathbf{k},\omega+\omega')\ . \tag{4}$$

The dynamically screened effective interaction $W(\omega)$ is analyzed in the Appendix and corresponds to the random-phase-approximation (RPA) formulation adapted to the narrow-band systems. It must be remembered that $W(\omega)$ is such that $W(t)$ is a real function. Then, the only poles of the integrand of (4) located in the upper half-plane are those of the Green function. Considering these points and orbitals compatible with the crystal symmetry, the integral in ω' yields

$$M_{ff'}(\omega)=-\delta_{ff'}\int_{-\infty}^{E_F}N_f(\varepsilon)W(\varepsilon-\omega)d\varepsilon\ , \tag{5}$$

where $N_f(\varepsilon)$ is the density of states of the interacting system corresponding to an f orbital. The $\delta_{ff'}$ of expression (5) allows us to treat the different symmetries independently. This is so even if the spin-orbit coupling is considered, because of the independence of the different terms in the self-energy. Equation (5) can be solved self-consistently and the first iteration is obtained by considering $N_f^0(\omega)$ instead of $N_f(\omega)$, $N_f^0(\omega)$ being the density of states (DOS) obtained from the LDF calculation.

The expression of the self-energy is then

$$\Sigma(\mathbf{r},\mathbf{r}',\omega)=\sum_f[Un+M_f(\omega)]f(\mathbf{r})f^*(\mathbf{r}')\ . \tag{6}$$

A new quasiparticle spectrum can be obtained from

$$[-\nabla^2+V_{\mathrm{MT}}^{(n)}(\underline{I}-\underline{P}_f)+V_{\mathrm{MT}}^{(0)}\underline{P}_f]\varphi_{\mathbf{k}\alpha}(\mathbf{r})+\int d^3r'\Sigma(\mathbf{r},\mathbf{r}',\varepsilon_{\mathbf{k}\alpha})\varphi_{\mathbf{k}\alpha}(\mathbf{r}')=\varepsilon_{\mathbf{k}\alpha}\varphi_{\mathbf{k}\alpha}(\mathbf{r})\ , \tag{7}$$

where $\underline{I}$ is the identity and $\underline{P}_f$ stands for the projection operator to the $l=3$ angular momentum subspace; $V_{\mathrm{MT}}^{(y)}$ is the muffin-tin potential calculated with y electrons in the f level of the rare-earth atoms; and the band Hamiltonian of the noninteracting system $\{[-\nabla^2+V_{\mathrm{MT}}^{(n)}(\underline{I}-\underline{P}_f)+V_{\mathrm{MT}}^{(0)}\underline{P}_f]\}$ excludes all $f-f$ repulsive interaction in the one-body potential, since it is considered through Σ_H.

Equation (7) can also be written as

$$[-\nabla^2+V_{\mathrm{MT}}(\mathbf{r})]\varphi_{\mathbf{k}\alpha}(\mathbf{r})+\int d^3r'\Sigma'(\mathbf{r},\mathbf{r}',\varepsilon_{\mathbf{k}\alpha})\varphi_{\mathbf{k}\alpha}(\mathbf{r}')=\varepsilon_{\mathbf{k}\alpha}\varphi_{\mathbf{k}\alpha}(\mathbf{r})\ . \tag{8}$$

In this equation, $-\nabla^2+V_{\mathrm{MT}}(\mathbf{r})$ is the full muffin-tin potential band Hamiltonian of the noninteracting system and $\Sigma'(\mathbf{r},\mathbf{r}',\varepsilon_{\mathbf{k}\alpha})$ is now

$$\Sigma'(\mathbf{r},\mathbf{r}',\varepsilon_{\mathbf{k}\alpha})=\sum_f\{[Un+M_f(\varepsilon_{\mathbf{k}\alpha})]-[V_{\mathrm{MT}}^{(n)}(\mathbf{r})-V_{\mathrm{MT}}^{(0)}(\mathbf{r})]\}f(\mathbf{r})f^*(\mathbf{r}')\ . \tag{9}$$

The difference $V_{\mathrm{MT}}^{(n)}(\mathbf{r})-V_{\mathrm{MT}}^{(0)}(\mathbf{r})$ gives the local Coulomb repulsion potential for an electron produced by the other $n-1$ electrons. Therefore, this difference should be close to $U(n-1)$ according to the meaning of U. This is not exact because the muffin-tin potential and U are obtained using different ways. However, we can in general find a real number x between $\frac{1}{2}$ and 1 such that the effects produced in the $\varepsilon_{\mathbf{k},\alpha}$ spectrum by the potential $U(n-x)$ or $V_{\mathrm{MT}}^{(n)}(\mathbf{r})-V_{\mathrm{MT}}^{(0)}(\mathbf{r})$ are similar when we solve (8). Then $\Sigma'(\mathbf{r},\mathbf{r}',\omega)$ in (8) can be approximated to

$$\Sigma'(\mathbf{r},\mathbf{r}',\omega)=\sum_f[Ux+M_f(\omega)]f(\mathbf{r})f^*(\mathbf{r}')\ , \tag{10}$$

with $\frac{1}{2}\le x\le 1$. x tends to 1 for f compounds with $n\gg 1$ and tends to $\frac{1}{2}$ for the Ce systems. In any case, the value of x can be approximately determined when the potentials $V_{\mathrm{MT}}^{(n)}(\mathbf{r})$ and $V_{\mathrm{MT}}^{(0)}(\mathbf{r})$ have been obtained. This value depends fundamentally on the amount of exchange and correlation included in $V_{\mathrm{MT}}^{(n)}(\mathbf{r})$ and $V_{\mathrm{MT}}^{(0)}(\mathbf{r})$. Therefore, in our method we consider an only fitting parameter which is that of the Kohn-Sham exchange functional.

Nevertheless, one can follow the inverse procedure considering the value of x as a fitting parameter and deducing after the value for the Kohn-Sham exchange parameter. The value of the U energy can be obtained from the available experimental data.

The effects of the $\Sigma'(\omega)$ potential on each symmetry can be analyzed by studying the intersection, for each energy ε_0, of the line $y_1=\omega-\varepsilon_0$ with the function $y_2=\mathrm{Re}[Ux+M_f(\omega)]$.[34-36] The energy interval of ε_0 obviously is the f bandwidth obtained within the LDF. Expression (10) produces the same effects as the first order self-energy corrections (Hartree-Fock approximations) in the limit case of those systems whose f symmetries are either totally occupied or totally empty. Actually, for the totally unoccupied f symmetries $M_f(\omega)=0$, and thus we obtain a single cut at $\omega=Ux$, which yields the upper Hubbard peak of the DOS. In the case of having a single f symmetry that is totally occupied and the others are completely unoccupied, $M_f(\omega)=-U$. Then, y_1 cuts off y_2 at $\omega=U(x-1)$. This single cut produces the lower Hubbard peak of the DOS. For the systems with partially occupied f symmetries, the corresponding $M_f(\omega)$'s present a variation versus ω as that of Fig. 1. Then, for each LDF state arising from a partially occupied orbital, there are three different resonances associated to the three different cuts of y_1 and y_2 (see Fig. 1). These three resonances, which have been experimentally observed[20-27] and theoretically discussed[1,11-16] in several Ce systems, cannot be reproduced with the first order self-energy theories. The unrestricted Hartree-Fock approximation locates each f orbital according to its own occupation[8,9] [in this case $M_f(\omega)=-Un_f$], and this can yield several peaks in the DOS. However, this last approximation obtains a state of the interacting system for each LDF state. Therefore, the electronic structure obtained from (10) differs both quantitatively and qualitatively from that obtained with a first order self-energy.

The former analysis allows us to obtain a schematic and partial pattern of the electronic structure of the HS which has been presented in a previous paper.[36] In this analysis we consider the heavy-fermion systems as an independent aggregation of rare-earth–actinide atoms and we suppose that their f orbitals are nonhybridized with other extended states. This is an oversimplified image of the HS, but it can give us some information about their electronic structures. However, if we want to obtain a realistic DOS to be compared with the experimental data, we should consider these systems as actual crystals in which the f states are hybridized.

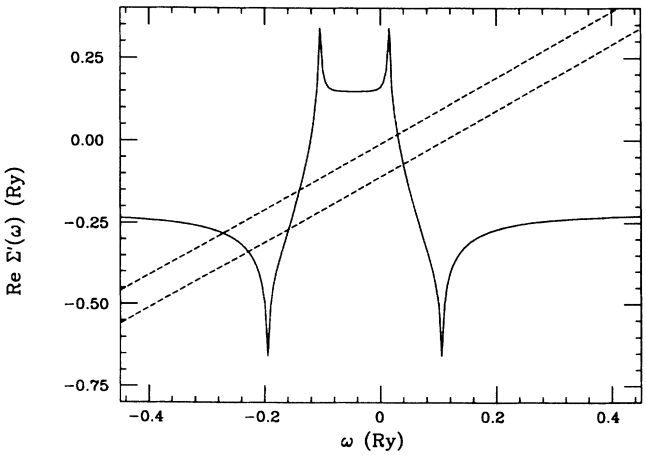

FIG. 1. Representation of $\mathrm{Re}\Sigma'(\omega)=[U/2+\mathrm{Re}M_f(\omega)]$ calculated for $n_f=0.9$ and $U=0.55$ Ry and the f width of the noninteracting system is 0.1 Ry. The dashed straight lines correspond to $y_1=\omega-\varepsilon_0$ and the separation between the two lines corresponds to the bandwidths determined by LDF (i.e., without considering self-energy corrections).

III. BAND CALCULATION METHOD

The influence of $\Sigma'(\mathbf{r},\mathbf{r}',\omega)$ in the $\varepsilon_{\mathbf{k},\alpha}$ band structure of the HS is the main objective of this work. In this work we consider realistic f states and thus the $\varepsilon_{\mathbf{k},\alpha}$ spectrum corresponds to states which contain several l orbital characters and only the f component of each state suffers the effects of $\Sigma'(\mathbf{r},\mathbf{r}',\omega)$.

We solve (8) using the APW method and the resulting matrix elements of the secular equation considering the self-energy operator,

$$[M_{ij}^{\alpha}(E)]_{\Sigma'}=[M_{ij}^{\alpha}(E)]_{\mathrm{APW}}+\sum_R X_j^{\alpha R}\sum_\nu Y_{ij}^{\nu R}Z_{ij}^{\nu R}(E)\ , \quad (11)$$

where

$$X_j^{\alpha R}=(4\pi)^2\frac{g}{n_\alpha}\Gamma_{11}^{\alpha}(R)\exp(i\mathbf{K}_j\cdot\mathbf{t}_R)\ , \quad (12)$$

$$Y_{ij}^{\nu R}=\frac{S_\nu^2}{\Omega}\exp[i(R^{-1}\mathbf{K}_j-\mathbf{K}_i)\cdot\mathbf{r}_\nu]I_3(K_iS_\nu)I_3(K_jS_\nu)\ , \quad (13)$$

$$Z_{ij}^{\nu R}(E)=\sum_f\left[\frac{d}{dr}\left[\ln\frac{R_3(\varepsilon_f,r)}{R_3(E,r)}\right]\right]_{r=S_\nu}\times\psi_f(\mathbf{K}_i)\psi_f(R^{-1}\mathbf{K}_j)\ , \quad (14)$$

with

$$\varepsilon_f=E-Ux-\mathrm{Re}M_f(E)\ , \quad (15)$$

where $\mathbf{K}_j=\mathbf{k}+\mathbf{G}_j$ ($\mathbf{G}_j$ is a reciprocal lattice vector); $\mathbf{t}_R$ is the nonprimitive lattice vector associated to the symmetry operation R (in the case of symmorphic symmetry group $\mathbf{t}_R=0$ for all R); g is the number of the symmetry operations of the group corresponding to the vector $\mathbf{k}$, n_α is the dimension of the irreducible representation α; the index ν runs over the rare-earth atoms of the primitive cell; Ω stands for the primitive cell volume; I_3 is the spherical Bessel function for $l=3$; S_ν is the muffin-tin radius of the ν atom whose position vector is $\mathbf{r}_\nu$; $\psi_f(\mathbf{K}_j)$ are linear combinations of $l=3$ orbitals compatible with the crystal symmetry and centered on the rare-earth–actinide atoms; $R_3(\varepsilon,r)$ is the radial part of the $l=3$ orbital calculated to the ε energy from the Schrödinger radial equation obtained within the augmented-plane-wave method;[37] $[M_{ij}^{\alpha}(E)]_{\mathrm{APW}}$ is the standard APW matrix elements corresponding to the irreducible representation α. The second term of the right

hand side of (11) can be interpreted as the equivalent pseudopotential arising from the self-energy operator between two ij APW basis. The band structure calculation described by expressions (11)–(15) is independent of the self-energy functional whenever this comes from a Hubbard Hamiltonian.

The energies E which satisfy the condition

$$\det\{[M_{ij}^{\alpha}(E)]_{\Sigma'}\}=0 \tag{16}$$

are eigenvalues which correspond to the eigenstates with a fixed $\mathbf{k}$ vector and α symmetry. On the other hand, the variable E in (16) is related with ε_f by means of (15). When one finds an eigenvalue E of the interacting HS, the corresponding ε_f is an energy of the noninteracting system. This means that ε_f is located in an energy interval (~ 1 eV) around the divergence of the logarithmic derivative of the function $R_3(\varepsilon,r)$ evaluated at $r=S_v$ and deduced with the Hamiltonian $[-\nabla^2+V_{\mathrm{MT}}(\mathbf{r})]$.

The energy spectrum deduced by using the band calculation method described in expressions (11)–(16) presents the following general features:

(i) The electronic states suffer the self-energy effects depending on their composition in f symmetries and each of these symmetries is independently shifted according to its M_f.

(ii) If an f orbital is totally unoccupied, $M_f(\omega)\rightarrow 0$. Then the corresponding bands are located at energies Ux and they are experimentally detected by inverse photoemission spectroscopy (IPS).[25]

(iii) For the case of occupied f symmetries, the self-energy presents large and sudden variations in the vicinity of the Fermi level, which produce the mass enhancements of the electronic states close to E_F as well as the large values of the electronic specific heat.

(iv) The effective shifts between eigenstates corresponding to the interacting and noninteracting systems are given by the energy differences between the zeros of equations: $\det\{[M_{ij}^{\alpha}(E)]_{\Sigma'}\}=0$ and $\det\{[M_{ij}^{\alpha}(E)]_{\mathrm{APW}}\}=0$. In general, the zeros corresponding to states with f component are located in an energy interval whose lower limit is an energy such that $[dR_3(r)/dr]=0$ for $r=S_v$ and the upper limit is the energy for which $R_3(r=S_v)=0$. The eigenstates of the interacting system are determined from Eq. (16) and in this case there are three energy intervals (per each partially occupied f orbital) in which states with f character can appear. Each of these intervals is centered in the energy of each of the cuts between the functions $y_1=E-\varepsilon_f$ and $y_2=Ux+\mathrm{Re}M_f(E)$ (see Fig. 1). The amount of the f character of each state increases as its energy approaches the upper limit of the corresponding energy interval. The effect of the self-energy (10) on an electronic state $|\mathbf{k}\alpha\rangle$ can be roughly estimated by

$$[Ux+\mathrm{Re}M_f(\varepsilon_{\mathbf{k}\alpha})]n_f(\varepsilon_{\mathbf{k}\alpha});[n_f(\varepsilon_{k\alpha})=|\langle \mathbf{k}\alpha|f\rangle|^2]$$

and this estimation can be evaluated in the same way at each step of the self-consistent process, although $M_f(\varepsilon_{\mathbf{k}\alpha})$, $n_f(\varepsilon_{\mathbf{k}\alpha})$, and $\varepsilon_{\mathbf{k}\alpha}$ can vary from step to step. It is interesting to remark that the effects of (10) on $\varepsilon_{\mathbf{k}\alpha}$ depend on $\mathbf{k}$ vector since the effective shifts for the states of the interacting system depend strongly on the momentum $\mathbf{k}$ because of the hybridization. As a consequence, sometimes, the number of zeros in (16) does not coincide with the number of cuts between the straight line $E-\varepsilon_{\mathbf{k}\alpha}^0$ and $\mathrm{Re}[\Sigma'(E)]$; instead, it corresponds to the cuts between the curves $(E-\varepsilon_{\mathbf{k}\alpha}^0)/n_f(E)$ and $\mathrm{Re}[\Sigma'(E)]$, $n_f(E)$ being the f component of the electronic state if it was located at the energy E. Therefore, the dependence of the effective shift on the momentum can produce breakings and discontinuities in the bands since for some $\mathbf{k}$'s the number of narrow resonances can be different from three. This is not surprising since the $\varepsilon_{\mathbf{k}\alpha}$ energies correspond to quasiparticle eigenstates. Therefore, we give the density of eigenstates, which are the solution of Eq. (8) as DOS.

(v) In this method the quasistates whose energies are obtained from Eq. (16) are affected by a mass enhancement defined by

$$\frac{m^*}{m_{\mathrm{LDF}}}\approx\left|1-\left[\sum_f n_f(\omega)\frac{\partial M_f(\omega)}{\partial\omega}\right]_{\omega=\mathrm{pole}}\right| . \tag{17}$$

Therefore m^*/m_{LDF} depends on the variations versus ω of $M_f(\omega)$ and $n_f(\omega)$. If one only considers a first order self-energy,[8,9] m^*/m_{LDF} is 1, since in these cases $M_f(\omega)=-U$. In the case described in this paper, m^*/m_{LDF} has sharp peaks in the energy interval where the real part of Σ' presents stronger variations (see Fig. 1). This precisely the energy interval where the three structures arising from the partially occupied f symmetry appear. Therefore the specific heat, which depends on m^*, will be large. This last property is an experimental feature which characterizes the heavy-fermion compounds and which a Hartree-Fock approximation to the self-energy cannot reproduce.

(vi) The imaginary part of the self-energy induces a quasiparticle character to these $|\mathbf{k}\alpha\rangle$ states and their lifetime can be approximately calculated by

$$\Gamma^{-1}\simeq\sum_f \mathrm{Im}M_f(\varepsilon_{\mathbf{k}\alpha})|\langle \mathbf{k}\alpha|f\rangle|^2 .$$

IV. COMMENTS ON THE RESULTS

We have considered α-$CeAl_2$ for testing our band calculation method for the following reasons:

(i) It is a clear heavy-fermion system whose electronic specific heat is ~ 150 mJ/mole $f$atom K^2 (this γ is ~ 15 times larger than, for instance, that of the α-Ce element[38]). This large specific heat is due to the narrowing effects in the structures just at E_F which can only be explained by the self-energy effects.

(ii) All studies of XPS detect an f structure at E_F and another about 2 eV below E_F (see, for instance, Refs. 20–27). In addition, the IPS obtains an f structure just above E_F and a giant f structure at ~ 5 eV above E_F.[24] Therefore α-$CeAl_2$ presents a structure of four f peaks which is clearly contradictory with the LDF calculations of the band structure.

(iii) The splitting of the double f structure below E_F cannot be attributed to spin polarization or to antiferromagnetic order since this compound shows a Pauli

paramagnetism.

(iv) The fourth reason for calculating the electronic structure of α-$CeAl_2$ is the strong hybridization suffered by the f states of this compound with *spd* states from both Ce and Al atoms. This hydridization allows us to probe our method in the most unfavorable conditions.

(v) At the present time, the theoretical analysis considering self-energy effects in the Ce compounds[1,11,13–16] has given schematic fDOS and only qualitative pictures of their electronic structure have been obtained.

The parameters for the band calculation are shown in Table I. The number of APW basis considered in this work is such that $|\mathbf{K}_i| \leq \sqrt{80}\pi/a$. The DOS and fDOS is performed using the standard methods.[39] The self-energy is determined using the dielectric function deduced in the Appendix. The DOS of the noninteracting system, considered for calculating $W(\omega)$, is that from the LDF. This DOS presents a giant f peak[40–42] at E_F without any splitting between the different f levels when both spin-orbit coupling and spin polarization effects are not considered. Then, the partial fDOS can be approximated by a square function in order to determine $\chi^0(\omega)$. In Ce compounds, the f electron count (n) is less than or equal to 1.[24,40–42] Therefore, the sum over f in expression (10) can be reduced to a single orbital (two in the case of spin-orbit coupling).

The DOS and fDOS calculated by LDF (Refs. 40 and 41) present evident discrepancies with the experimental data of XPS and IPS since the three peaks corresponding to the partially occupied f symmetry and the unoccupied f states located around 5 eV above E_F are not found in these calculations. In addition, there is not any f structure below E_F (at $\sim$2 eV).[39] However, n_{LDF} is in agreement with the XPS and IPS measurements.

Figure 2 shows the density of eigenstates deduced from Eq. (16) by considering the dynamically screened exchange potential [this is the denomination in the Hedin-Lundqvist theory[34] of a Σ' functional as that of expression (10)]. This DOS presents four peaks [see Fig. 2(b)], located at $\sim$0.54, $\sim$0.67, $\sim$0.84, and $\sim$1.1 Ry. The average values of m^*/m_{LDF} in these peaks are $\sim$1.3, $\sim$6.2, $\sim$7.5, and $\sim$1, respectively. Using the Fermi liquid argument, the specific heat enhancement is related to the enhancement of the quasiparticle density of states at the Fermi surface;[28] therefore, the relation γ/γ_0 deduced from our results can be estimated around 6. The three narrow structures [see Fig. 2(b)] come from the orbital xyz/r^3 and the Fermi level lies just in the second peak. The other two peaks of this group are located at $\sim$1.8 eV below E_F and $\sim$2.2 eV above E_F. The fourth

TABLE I. Different parameters used in the determination of the band structure: a is the lattice parameter; $\alpha_{\mathrm{Ce}}(\alpha_{\mathrm{Al}})$ stands for the α parameter of the Kohn-Sham local exchange potential, included in muffin-tin potential V_{MT}, corresponding to Ce(Al) ions; $S_{\mathrm{Ce}}(S_{\mathrm{Al}})$ is the muffin-tin radius corresponding to Ce(Al) ions.

a (a.u.)	α_{Ce}	α_{Al}	S_{Ce} (a.u.)	S_{Al} (a.u.)
14.77	2.11	2.00	2.91	2.39

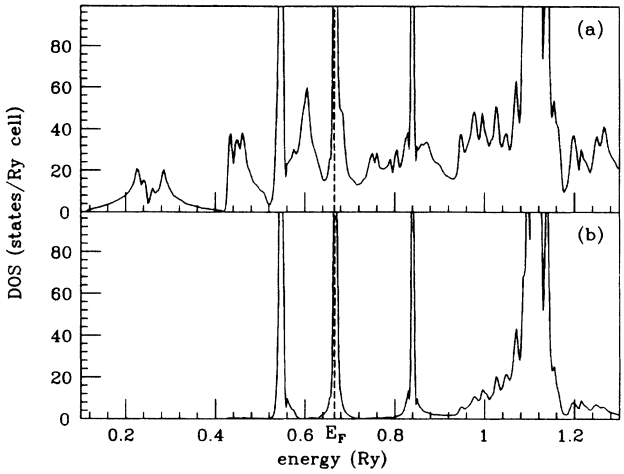

FIG. 2. Density of states calculated with $M_f(\omega)$ of expression (5) and $U=0.55$ Ry. (a) Total density of states. (b) Partial f density of states.

structure is a giant peak arising from the totally unoccupied f orbitals and located at $\sim$6 eV above E_F.

In a recent paper,[43] we have calculated the electronic structure of $CeAl_2$ by considering a first order self-energy correction. The electronic structure obtained by this method presents just two f peaks in the DOS, one of them below E_F and the other above. Although the electronic structure of Ref. 43 corresponds to the γ phase of $CeAl_2$ and the results of Fig. 2 to the α phase of this compound, we can compare both results since as it is well known[14–16,20–23] the electronic structure of these two phases are qualitatively equal and quantitatively similar. The main conclusion that can be drawn is that, as we have already commented in Sec. II, the dynamical effects included by $M_f(\omega)$ in (10) produce the splitting of the peak arising from the xyz/r^3 orbital in the narrow resonances shown in Fig. 2(b). This effect is also described by Zlatić *et al.*,[1] who study the case of only one f symmetry. They find that the fDOS of the noninteracting system is split in three resonances when the self-energy is considered, two of them symmetrically located with respect to E_F and the other structure lying just at E_F. The most significative difference is that in our calculation the narrow resonances are not in total symmetry with respect to E_F. This difference can be caused by the different approximations used for the self-energy. Martin[11] concludes that three or four resonances should appear in the interacting system for each f symmetry of the noninteracting system. He argues that a fourth peak in the fDOS can arise if the hybridization with other extended states of the resonance located at E_F produces a gap (or pseudogap) in the total DOS. Therefore, our results are also consistent with this provision of Martin's model, although in this compound the hybridization does not produce any gap at E_F. There are other theoretical studies of the fDOS of the Ce compounds performed with different self-energy approximations[14–16] and they all present a peak below E_F (around -2 eV) and another peak just at E_F.

The XPS results given in Refs. 20–23 present two f peaks, one of them ~ 2 eV below E_F and the other close to E_F. The relatively large specific heat of this compound[38] implies the existence of a mass enhancement of the states located at E_F. Therefore our results are basically consistent with these data. The fDOS [Fig. 2(b)] presents a peak at ~ 2.2 eV above E_F and another one at ~ 6 eV, which qualitatively agrees with the IPS experiments.[24,25] However, the widths of the structures at -1.8 eV and $+6$ eV from E_F [Fig. 2(b)] do not coincide with the XPS and IPS results, respectively. This discrepancy can be attributed to the relaxation effects that arise in the high energy spectroscopy process.

In summary, we have given a calculation method which determines the DOS and fDOS from band structure. This method has been applied to a Ce system and we have used it for explaining the different splittings between the strong correlated bands, schematically foreseen in several former papers[1,11–16] but never deduced hitherto from a band structure calculation. This method can also be valid for the uranium compounds, although application to these materials requires the consideration of several symmetries in Eqs. (A3) and (10) since n is ~ 2.5. However, the calculation procedure is similar.

APPENDIX

We start from the bare interaction given in Eq. (5) of our previous paper[8] and the dielectric function $\varepsilon(\omega)$ is deduced from the RPA integral equation adapted to the Hubbard systems,

$$\sum_{f,f'} |f\rangle_1|f'\rangle_2 W(\mathbf{q},\omega)\langle f|_1\langle f'|_2 = U \sum_{f,f'} |f\rangle_1|f'\rangle_2\langle f|_1\langle f'|_2 - iU \sum_{f,f'} \frac{1}{N} \sum_{\mathbf{k},\alpha,\beta} \sum_{f''} |\langle \mathbf{k}+\mathbf{q}\beta|f''\rangle|^2 |\langle \mathbf{k}\alpha|f''\rangle|^2 \int \frac{d\omega'}{2\pi} G^0_\beta(\mathbf{k}+\mathbf{q},\omega+\omega') G^0_\alpha(\mathbf{k},\omega') \times |f\rangle_1|f'\rangle_2 W(\mathbf{q},\omega)\langle f|_1\langle f'|_2 \ . \quad \text{(A1)}$$

The dependence of $W(\mathbf{q},\omega)$ on the momentum $\mathbf{q}$ is given by means of the $\chi(\mathbf{q},\omega)$ and it is well known[28] that the χ function is, in heavy-fermion systems, independent of $\mathbf{q}$ and strongly dependent on ω. Therefore, we assume that the momentum dependence of the dynamically screened interaction is negligible compared with the energy dependence and thus, we substitute $W(\mathbf{q},\omega)$ by $(1/N)\sum_{\mathbf{q}} W(\mathbf{q},\omega)$. Then Eq. (A1) is

$$W(\omega) = U[1 - U\chi^0(\omega)]^{-1} \ , \quad \text{(A2)}$$

where

$$\chi^0(\omega) = \sum_f \int_{-\infty}^{0} d\varepsilon \int_0^{\infty} d\varepsilon' N_f^0(\varepsilon) N_f^0(\varepsilon') \left[\frac{1}{\omega+\varepsilon-\varepsilon'+i\theta} - \frac{1}{\omega-\varepsilon+\varepsilon'+i\theta} \right] , \quad \text{(A3)}$$

and where $N_f^0(\varepsilon)$ is the noninteracting system density of states corresponding to the f orbital.

When the process is performed self-consistently, this last expression can give $\chi(\omega)$ by substituting N_f^0 for N_f. If one considers a square function N_f^0 for each orbital, $\chi^0(\omega)$ is

$$\begin{aligned}\chi^0(\omega) = -\sum_f N_{0f}^2 \{ &(\omega+\Delta_f)\ln|\omega+\Delta_f| - (\omega-\Delta_f)\ln|\omega-\Delta_f| \\ &-(\omega+b_f)\ln|\omega+b_f| + (\omega-b_f)\ln|\omega-b_f| - (\omega+a_f)\ln|\omega+a_f| + (\omega-a_f)\ln|\omega-a_f| \\ &+ i\pi \,\mathrm{sgn}(\omega)\{ b_f[\Theta(\omega-b_f)-\Theta(\omega-\Delta_f)+\Theta(-\omega-b_f)-\Theta(-\omega-\Delta_f)] \\ &+ a_f[\Theta(\omega-a_f)-\Theta(\omega-\Delta_f)+\Theta(-\omega-a_f)-\Theta(-\omega-\Delta_f)] \\ &+ \omega[\Theta(\omega)-\Theta(\omega-b_f)-\Theta(\omega-a_f)+\Theta(\omega-\Delta_f) \\ &-\Theta(-\omega)+\Theta(-\omega-b_f)+\Theta(-\omega-a_f)-\Theta(-\omega-\Delta_f)]\}) \ , \end{aligned} \quad \text{(A4)}$$

where N_{0f} is the constant density of states corresponding to the f orbital, $\Delta_f = N_{0f}^{-1}$ is the bandwidth, and $a_f = n_f\Delta_f$ [$b_f = (1-n_f)\Delta_f$] is the occupied (unoccupied) energy interval of the f orbital, $\Theta(x)$ is the step function.

The dielectric function is then

$$\varepsilon(\omega) = 1 - U\chi^0(\omega) = \varepsilon_1(\omega) + i\varepsilon_2(\omega) \ . \quad \text{(A5)}$$

The function $\varepsilon(\omega)$ given in (A4) is very sensible before changes of the three main electronic parameters of the heavy-fermion systems (Δ, n, and U). For $\omega \to 0$, $\varepsilon_1(\omega)$ is positive and sharply decreases for increasing ω. One of the most important characteristics of $\varepsilon_1(\omega)$ is that it presents two zeros for $\omega > 0$ (and two symmetric zeros on the negative real axis) which correspond to peaks of the effective interaction $W(\omega)$. At the first zero, $\varepsilon_2(\omega) \neq 0$, and at the second one $\varepsilon_1(\omega)$ and $\varepsilon_2(\omega)$ are both vanishing (this last zero is assigned to the free plasmon pole).

[1]V. Zlatić, S. K. Ghatak, and K. H. Bennemann, Phys. Rev. Lett. **57**, 1263 (1986).
[2]R. Blankenbecler, J. R. Fulco, W. Gill, and D. J. Scalapino, Phys. Rev. Lett. **58**, 411 (1987).
[3]R. W. Godby and P. J. Needs, Phys. Rev. Lett. **62**, 1169 (1989).
[4]In-Whan Lyo and E. W. Plummer, Phys. Rev. Lett. **60**, 1558 (1988).
[5]G. Teglia, F. Duclastle, and D. Spanjard, Phys. Rev. B **21**, 3729 (1980).
[6]J. P. Perdew and M. Levy, Phys. Rev. Lett. **51**, 1884 (1983).
[7]L. J. Sham and M. Schluter, Phys. Rev. Lett. **51**, 1888 (1983).
[8]F. López-Aguilar and J. Costa-Quintana, J. Phys. C **20**, 2485 (1986); S. Balle, J. Costa-Quintana, and F. López-Aguilar, *ibid.* **20**, L223 (1987).
[9]P. Thalmeier and L. M. Falicov, Phys. Rev. B **22**, 2456 (1980); G Czycholl, Phys. Rep. **143**, 277 (1986); S. Balle, J. Costa-Quintana, and F. López-Aguilar, Phys. Rev. B **37**, 6615 (1988).
[10]W. E. Picket, Rev. Mod. Phys. **61**, 433 (1989).
[11]R. M. Martin, Phys. Rev. Lett. **48**, 362 (1982).
[12]J. W. Allen and R. M. Martin, Phys. Rev. Lett. **49**, 1106 (1982).
[13]R. M. Martin and J. W. Allen, in *Valence Fluctuations in Solids*, edited by L. M. Falicov, W. Hanke, and M. B. Maple (North-Holland, Amsterdam, 1981), p. 85.
[14]S. H. Liu and K. M. Ho, Phys. Rev. B **26**, 7052 (1982).
[15]T. Watanabe and A. Sakuma, Phys. Rev. B **31**, 6320 (1985).
[16]M. D.Nuñez-Ruguiero and M. Avignon, Phys. Rev. Lett. **55**, 615 (1985).
[17]B. I. Min, H. J. F. Jansen, T. Oguchi, and A. J. Freeman, Phys. Rev. B **34**, 369 (1986).
[18]N. Sivan and Z. Zinamon, Phys. Rev. B **37**, 5535 (1988).
[19]E. Louis, J. A. Vergés, and F. Flores, Phys. Rev. B **34**, 6415 (1986).
[20]D. M. Wieliczka, C. G. Olson, and W. Linch, Phys. Rev. Lett. **52**, 2180 (1984).
[21]D. M. Wieliczka, C. G.Olson, and W. Linch, Phys. Rev. B **29**, 3028 (1984).
[22]M. Croft, J. H. Weaver, D. J. Peterman, and F. Franciosi, Phys. Rev. Lett. **46**, 1104 (1981).
[23]J. W. Allen, S. J. Oh, I. Lindau, J. M. Lawrence, L.I. Johansson, and S. B. Hagstrom, Phys. Rev. Lett. **46**, 1100 (1981).
[24]E. Wuillord, H. R. Moser, W. D. Schneider, and Y. Baer, Phys. Rev. B **28**, 7354 (1983).
[25]Y. Baer, H. R. Ott, J. C. Fuggle, and L. E. deLong, Phys. Rev. B **24**, 5384 (1981).
[26]R. D. Parks, S. Raen, M. L. denBoer, Y. S. Chang, and G. P. Williams, Phys. Rev. Lett. **52**, 2176 (1984).
[27]F. Pattley, B. Delley, W. Schneider, and Y. Baer, Phys. Rev. Lett. **55**, 1518 (1985).
[28]C. M. Varma, Phys. Rev. Lett. **55**, 2723 (1985).
[29]T. M. Rice, J. Magn. Magn. Mater. **63-64**, 689 (1987).
[30]C. S. Wang, H. Krakauer, and W. E. Pickett, J. Phys. F **16**, L287 (1986).
[31]T. Oguchi, A. J. Freeman, and G. W. Crabtree, Phys. Lett. A **117**, 428 (1986).
[32]C. S. Wang, M. R. Norman, R. C. Albers, A. M. Boring, W. E. Pickett, H. Krakauer, and N. E. Christensen, Phys. Rev. B **35**, 7260 (1987).
[33]L. Taillefer and G. G. Lonzarich, Phys. Rev. Lett. **60**, 1570 (1988).
[34]L. Hedin and S. Lundqvist, Solid State Phys. **23**, 2 (1969).
[35]A. Liebsch, Phys. Rev. B **23**, 5203 (1981).
[36]F. López-Aguilar, S. Balle, and J. Costa-Quintana, Phys. Rev. B **39**, 9591 (1989).
[37]This method allows us to calculate f orbitals for different energies which are truncated at $r = S_v$. Alternative solutions of the f orbitals of (14) are those arising from the RAA method. The only difference between the solutions of these two methods is the truncation radii of the radial functions, since in the RAA method, S_v is substituted by the equivalent Wigner radius r_{ws}. However, the consideration of the orbitals arising from the RAA method implies a large complexity in this band structure method and does not ensure any improvement in the results.
[38]G. P. Meisner, A. L. Giorgi, A. C. Lawson, G. R. Stewart, J. O. Willis, M. S. Wire, and J. L. Smith, Phys. Rev. Lett. **53**, 1829 (1984).
[39]A. H. McDonald, S. H. Vosko, and P. T. Coleridge, J. Phys. C **12**, 2991 (1979).
[40]T. Jarlborg, A. J. Freeman, and D. D. Koelling, J. Phys. (Paris) **43**, C7-317 (1982).
[41]F. López-Aguilar and J. Costa-Quintana, Phys. Status Solidi B **132**, 485 (1985).
[42]W. E. Pickett and B. M. Klein, J. Less-Common Met. **93**, 219 (1983).
[43]F. López-Aguilar, J. Costa-Quintana, and S. Balle, Phys. Status Solidi B **152**, 543 (1989).